Figs1

A

Recessive model (based on 2 copies of APOL1 risk variants) --age-gender-gfr -10PCs

Clinical Phenotype/diagnosis	Cases	Controls	Odds Ratio (95% CI)	p-value
Infection/inflammation of internal prosthetic device or graft	371	52431	1.38 (1.06-1.80)	0.02
Septicemia	800	46455	1.19 (0.98-1.44)	0.08
Sepsis and SIRS	320	53247	1.45 (1.08-1.93)	0.01
Sepsis	274	53247	1.37 (1.10-1.88)	0.05

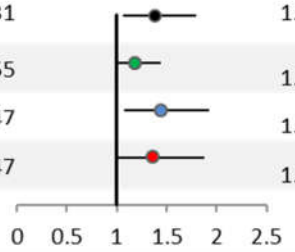

B

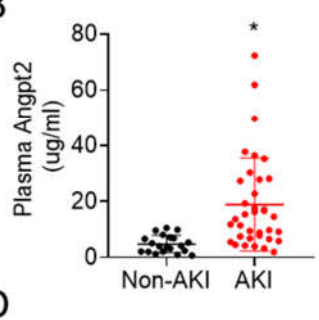

C

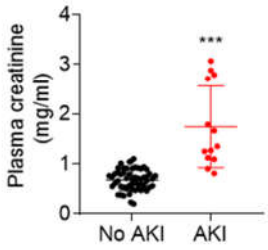

D

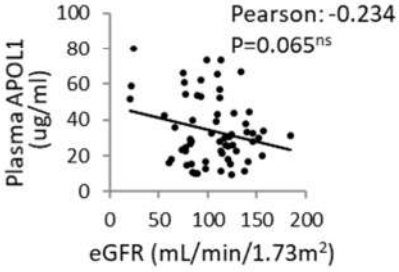

E

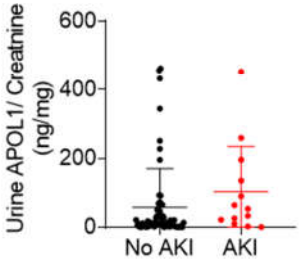

F

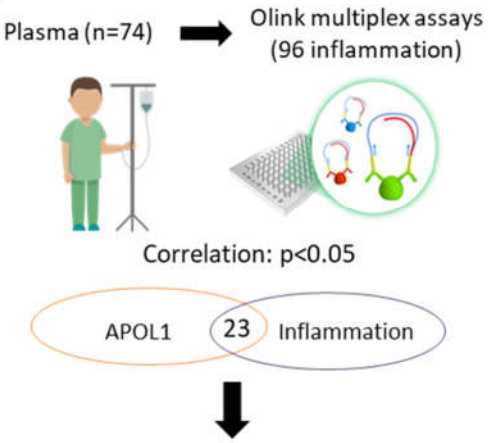

Name	P value	Name	P value	Name	P value				
IL-8	0.088	**CXCL9**	0.01	TWEAK	0.293	CD70	0.768	LAMP3	0.158
TNFRSF9	0.11	**CD8A**	0.037	**PDGF.subunit.B**	0.002	IL10	0.413	CASP.8	0.453
TIE2	0.856	**CAIX**	0.046	PDCD1	0.131	**TFNRSF12A**	0.012	ICOSLG	0.128
MCP.3	0.001	**MUC.16**	0.019	FASLG	0.262	CCL23	0.085	MMP12	0.882
CD40.L	0.035	**ADA**	0.041	IL12	0.631	CD5	0.464	CXCL13	0.104
CD244	0.006	CD4	0.496	CCL19	0.738	CCL3	0.883	PD.L2	0.62
EGF	0.001	NOS3	0.444	MCP.2	0.056	MMP7	0.157	VEGFA	0.525
ANGPT2	0.006	CD83	0.187	CCL4	0.663	ARG1	0.386	IL4	0.356
IL7	0.164	**Gal.9**	0.006	IL15	0.074	NCR1	0.36	LAG3	0.276
PGF	0.071	**VEGFR.2**	0.016	Gal.1	0.798	DCN	0.062	IL12RB1	0.559
IL6	0.037	CD40	0.686	CD27	0.075	TNFRSF21	0.052	IL13	0.103
ADGRG1	0.549	IL18	0.239	**CXCL5**	0.004	TNFRSF4	0.058	TNF	0.19
MCP.1	0.065	GZMH	0.094	IL-5	0.944	MIC.A.B	0.674	KLRD1	0.197
CRTAM	0.14	KIR3DL1	0.663	**HGF**	0.02	**CCL17**	0.005	GZMB	0.413
CXCL11	0.566	**LAP.TGF.beta.1**	0.009	GZMA	0.663	ANGPT1	0.813		
MCP.4	0.417	**CXCL1**	0.023	HO.1	0.291	PTN	0.062		
TRAIL	0.004	TNFSF14	0.732	CX3CL1	0.985	**CXCL12**	0.027		
PD.L1	0.315	**CSF.1**	0.023	CXCL10	0.243	IFN.gamma	0.415		

Figure S1. Plasma APOL1 level in patients with COVID19 correlates with markers of endothelial dysfunction and kidney disease severity. Related to Figure 1.

A. Association between *APOL1* risk alleles (recessive model) and sepsis phenotypes in the MVP cohort. All analyses were adjusted for age, sex, GFR and ancestry.
B. Plasma ANGPT2 levels in patients with and without AKI in the MESSI cohort. *p<0.05.
C. Plasma creatinine levels in AKI and non-AKI event (74 samples from 30 individuals) in the COVID19 study. AKI events were defined according to KDIGO criteria. ***p<0.001.
D. The correlation between plasma APOL1 level and eGFR.
E. Urine APOL1 levels in No AKI and AKI samples. ns: not statistically significant.
F. O-link inflammation panel target 92 inflammation-related protein biomarkers. The proteins highlighted in red significantly related to APOL1 level.

Figs2

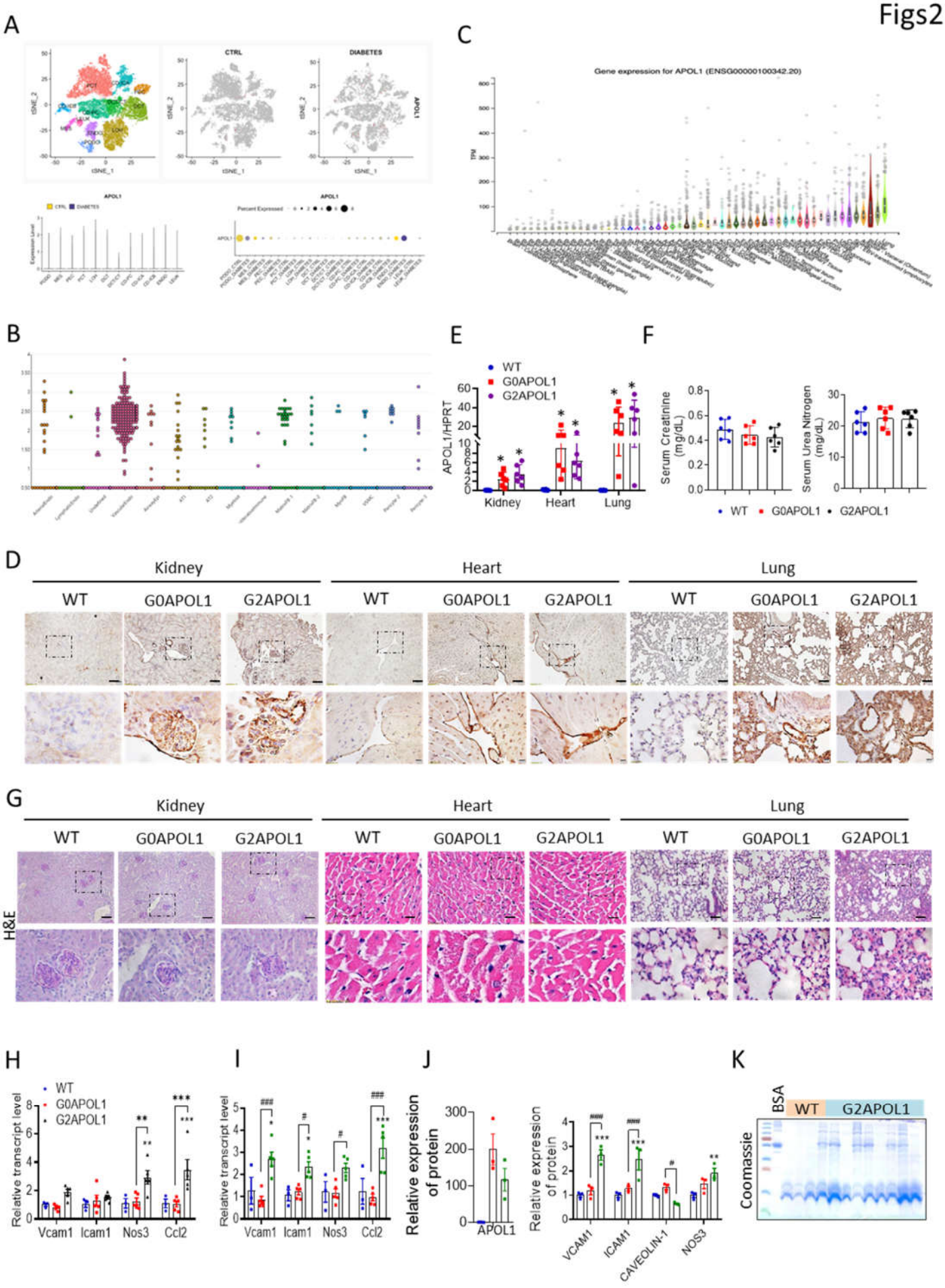
A
CTRL
DIABETES
APOL1
C
Gene expression for APOL1 (ENSG00000100342.20)
TPM
B
E
WT
G0APOL1
G2APOL1
APOL1/HPRT
Kidney
Heart
Lung
F
Serum Creatinine (mg/dL)
Serum Urea Nitrogen (mg/dL)
WT
G0APOL1
G2APOL1
D
Kidney
Heart
Lung
WT
G0APOL1
G2APOL1
G
H&E
H
Relative transcript level
Vcam1
Icam1
Nos3
Ccl2
I
J
Relative expression of protein
APOL1
VCAM1
ICAM1
CAVEOLIN-1
NOS3
K
BSA
WT
G2APOL1
Coomassie

Figure S2: Generation of a mouse model with cell-type-specific inducible expression of *APOL1* variants. Related to Figure 2.

A. Single cell expression distribution of *APOL1* in human kidney. Data downloaded from Humphreys lab (https://humphreyslab.com)
B. Single cell expression distribution of *APOL1* in human lung. Data downloaded from LungGENS database (https://research.cchmc.org/pbge/lunggens/default.html);
C. *APOL1* expression in different human tissue samples. Data was downloaded from GTEX database (www. Gtex.org)
D. Immunohistochemical analysis of green fluorescent protein (GFP) in the kidney, heart and lung of WT, EC/*G0APOL1* and EC/*G2APOL1* mice. Brown staining indicates GFP expression. Scale bar =20 µM.
E. Relative APOL1 transcript level in kidneys of *WT* (N = 5), EC/*G0APOL1* (N = 6) and EC/*G2APOL1* (N = 6) mice. APOL1 mRNA level is normalized to HPRT; *p<0.05, vs WT.
F. Serum creatinine and urea nitrogen levels in *WT* (N = 6), EC/*G0APOL1* (N = 6), and EC/*G2APOL1* mice. ns - not statistically significant.
G. Representative images of H&E-stained lung, kidney and heart section from *WT,* EC/*G0APOL1* and EC/*G2APOL1* mice. Scale bar=20 µm.
H. Relative mRNA levels of Vcam1, Icam1, Nos3, and Ccl2 were evaluated in hearts of WT (N = 3), EC/G0APOL1 (N = 5) and EC/G2APOL1 (N = 5) mice.; **p<0.01, ***p<0.001 vs *WT*; $^{\#\#}$p < 0.01, $^{\#\#\#}$p < 0.001 vs. indicated group.
I. Relative mRNA levels of Vcam1, Icam1, Nos3, and Ccl2 were evaluated in lungs of WT (N = 3), EC/G0APOL1 (N = 5) and EC/G2APOL1 (N = 5) mice.; *p<0.05, ***p<0.001 vs *WT*; $^{\#}$p < 0.05, $^{\#\#\#}$p < 0.001 vs. indicated group.
J. Densitometric quantification of levels of APOL1 Icam1, Vcam1, Caveolin-1, and eNOS normalized to GAPDH in lung tissues of WT, EC/*G0APOL1* and EC/*G2APOL1* mice as shown in Figure 1I. N = 3 independent experiments; **p<0.01, ***p<0.001 vs *WT*.
K. Comassie blue-stained SDS-PAGE gel of urine samples from WT (N = 3), and EC/*G2APOL1* (N = 9) mice.

Figs3

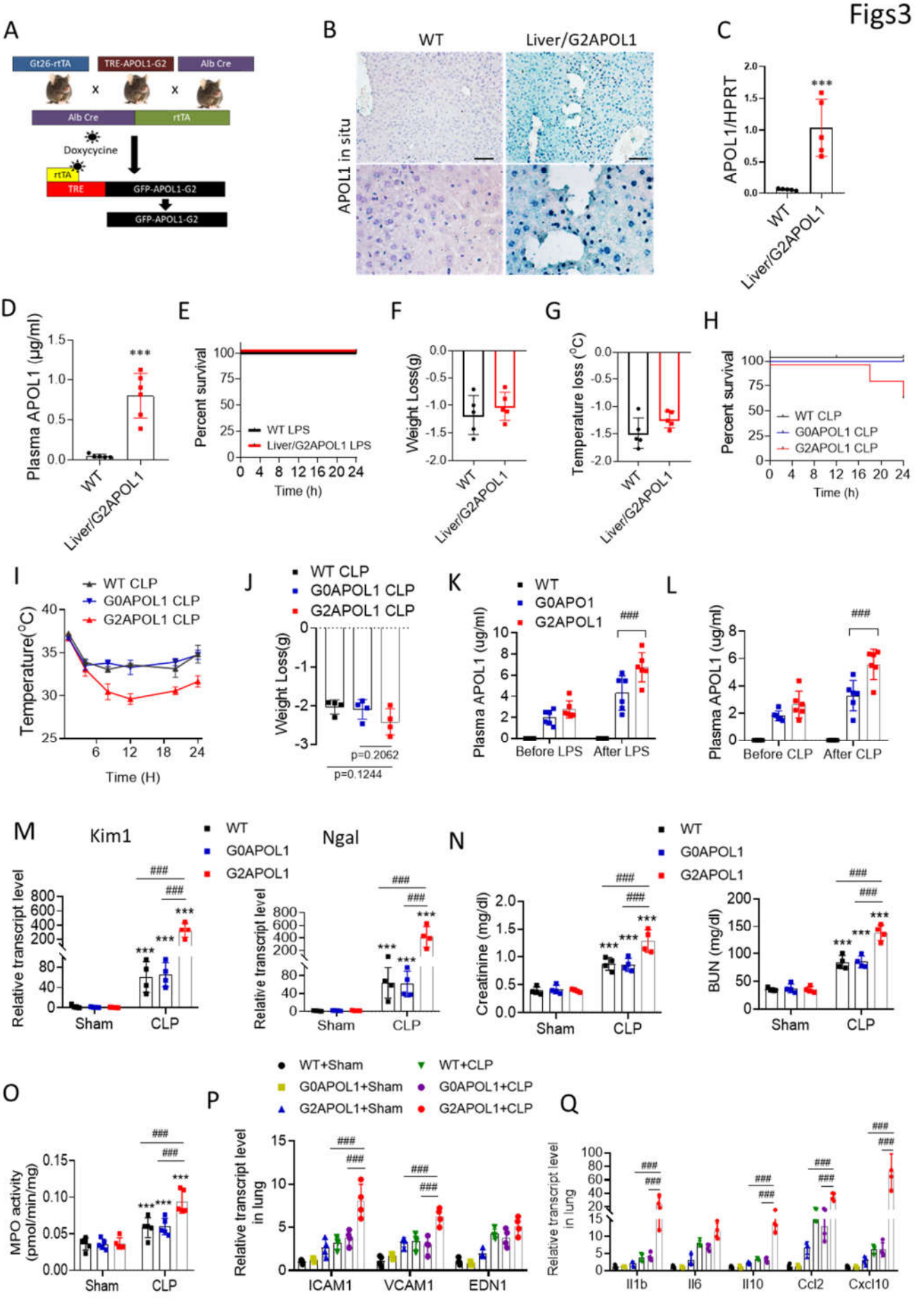
A
Gt26-rtTA
TRE-APOL1-G2
Alb Cre
Alb Cre
rtTA
Doxycycine
rtTA
TRE
GFP-APOL1-G2
GFP-APOL1-G2
B
WT
Liver/G2APOL1
APOL1 in situ
C
APOL1/HPRT
WT
Liver/G2APOL1
D
Plasma APOL1 (μg/ml)
WT
Liver/G2APOL1
E
Percent survival
WT LPS
Liver/G2APOL1 LPS
Time (h)
F
Weight Loss(g)
WT
Liver/G2APOL1
G
Temperature loss (°C)
WT
Liver/G2APOL1
H
Percent survival
WT CLP
G0APOL1 CLP
G2APOL1 CLP
Time (h)
I
WT CLP
G0APOL1 CLP
G2APOL1 CLP
Temperature(°C)
Time (H)
J
WT CLP
G0APOL1 CLP
G2APOL1 CLP
Weight Loss(g)
p=0.2062
p=0.1244
K
WT
G0APO1
G2APOL1
Plasma APOL1 (ug/ml)
Before LPS
After LPS
L
Plasma APOL1 (ug/ml)
Before CLP
After CLP
M
Kim1
Ngal
WT
G0APOL1
G2APOL1
Relative transcript level
Sham
CLP
N
WT
G0APOL1
G2APOL1
Creatinine (mg/dl)
BUN (mg/dl)
Sham
CLP
O
MPO activity (pmol/min/mg)
Sham
CLP
P
WT+Sham
G0APOL1+Sham
G2APOL1+Sham
WT+CLP
G0APOL1+CLP
G2APOL1+CLP
Relative transcript level in lung
ICAM1
VCAM1
EDN1
Q
Relative transcript level in lung
Il1b
Il6
Il10
Ccl2
Cxcl10

Figure S3. Increased sepsis severity in endothelial EC/*G2APOL1* mice. Related to Figure 3.

A. Experimental design for the generation of the *Gt26-rtTA/TREG2APOL1-GFP /Alb Cre (Liver/G2APOL1)* mice.
B. Representative images of APOL1 in situ hybridization in liver of WT and liver/*G2APOL1* mice. Scale bar=100 μm.
C. Relative APOL1 transcript level in liver of WT (N = 5) and Liver/*G2APOL1* (N = 5) mice. APOL1 mRNA level is normalized to HPRT; ***p<0.001, vs WT.
D. Plasma APOL1 level in WT (N=5) and Liver/*G2APOL1* (N=6) mice. ***p<0.001, vs WT.
E. Survival following intraperitoneal injection of LPS (6mg/kg) in WT (N=5) and Liver/*G2APOL1* (N=5) mice.
F. Weight loss after intraperitoneal injection of LPS (6mg/kg) at 24h in WT (N=5) and Liver/*G2APOL1* (N=5) mice.
G. Body temperature response to saline or LPS in WT (N=5) and Liver/*G2APOL1* (N=5) mice.
H. Survival after cecal ligation and puncture (CLP) or sham operation in WT (N = 4), EC/*G0APOL1* (N = 4) and EC/*G2APOL1* (N = 8) mice.
I. Rectal temperature in CLP or sham operated WT, EC/*G0APOL1* and EC/*G2APOL1* mice.
J. Weight loss after 24 hours of CLP or sham operation of WT, EC/*G0APOL1* and EC/*G2APOL1* mice.
K. Serum APOL1 was measured at the time or 24 hours after LPS injection in WT, EC/*G0APOL1* and EC/*G2APOL1* mice; ###p < 0.001 vs. indicated group.
L. Serum APOL1 was measured either before or 24 hours after CLP operation in WT, EC/*G0APOL1* and EC/*G2APOL1* mice; ###p < 0.001 vs. indicated group.
M. Relative transcript level of AKI injury markers; Kidney injury Kim1 and Ngal in the kidneys of control (N = 4), EC/ *G0APOL1* (N = 4) and EC/*G2APOL1* (N = 4) mice; ***p<0.001 vs *sham*; $^{###}$p < 0.001 vs. indicated group.
N. Renal function of WT, EC/*G0APOL1* and EC/*G2APOL1* mice 24hour after either CLP or sham operation in WT (N = 4), EC/*G0APOL1* (N = 4) and EC/*G2APOL1* (N = 4) mice, assessed by serum BUN and creatinine. ***p<0.001 vs *sham*; $^{###}$p < 0.001 vs. indicated group.
O. MPO activity was measured at 24 hours in lungs of mice undergoing CLP or sham operation in WT (N=4), EC/*G0APOL1* (N = 4) and EC/*G2APOL1* (N=4) mice; **p<0.01 and ***p<0.001 vs *sham*; $^{##}$p < 0.01 vs. indicated group.
P. Relative mRNA levels of Vcam1, Icam1, and Edn1 were evaluated in lungs of WT (N = 4), EC/*G0APOL1* (N = 4) and EC/*G2APOL1* (N = 4) mice; ***p<0.001 vs *WT*; $^{#}$p < 0.05, $^{##}$p < 0.01, $^{###}$p < 0.001 vs. indicated group.
Q. Relative mRNA levels of Il1b, Il6, Il10, Ccl2 and Cxcl10 in lungs of WT (N = 4), EC/*G0APOL1* (N = 4) and EC/*G2APOL1* (N = 4) mice.; **p<0.01, ***p<0.001 vs *WT*; $^{##}$p < 0.01, $^{###}$p < 0.001 vs. indicated group.

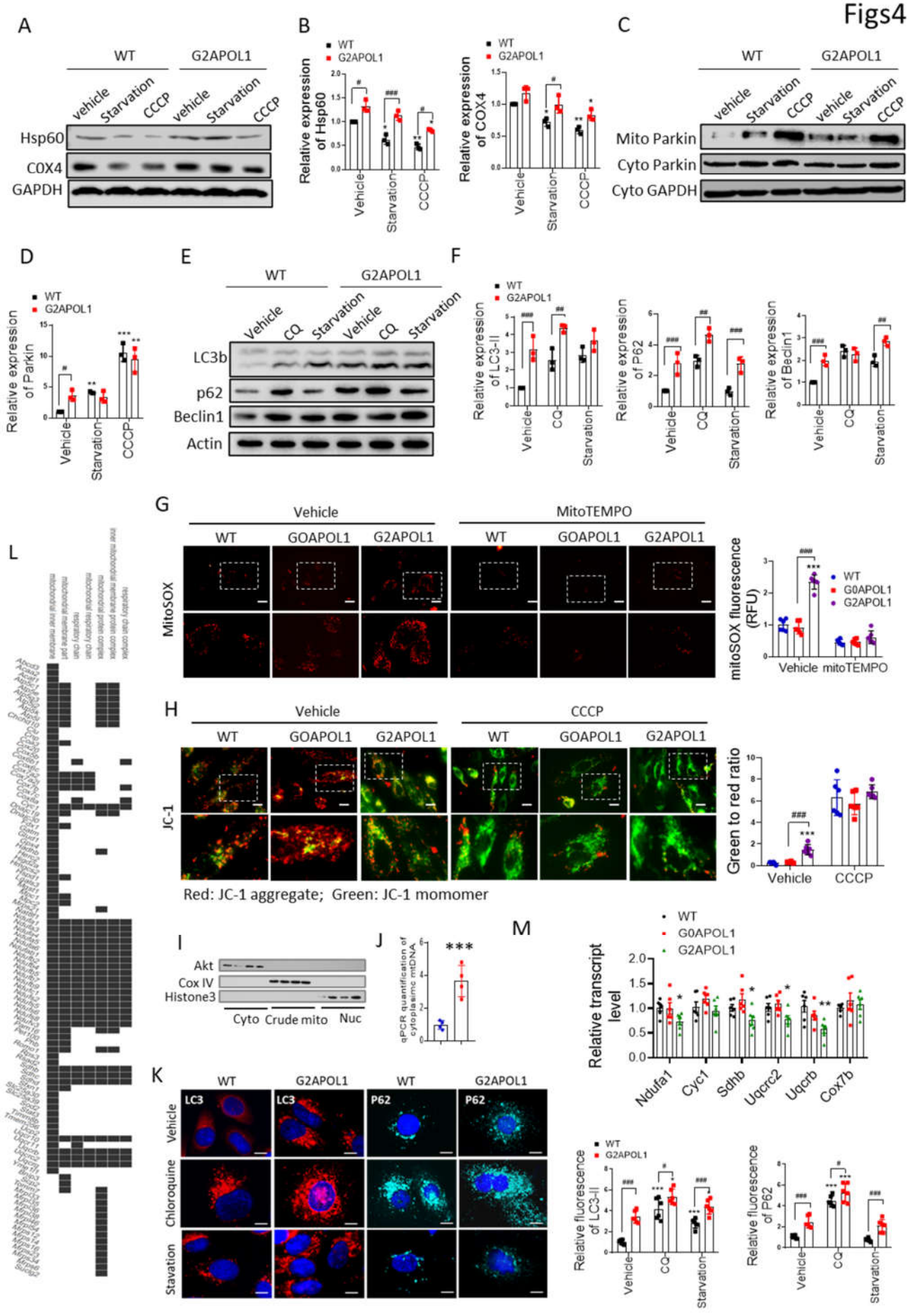
Figs4
A
WT
G2APOL1
vehicle
Starvation
CCCP
Hsp60
COX4
GAPDH
B
Relative expression of Hsp60
Relative expression of COX4
C
Mito Parkin
Cyto Parkin
Cyto GAPDH
D
Relative expression of Parkin
E
LC3b
p62
Beclin1
Actin
CQ
F
Relative expression of LC3-II
Relative expression of P62
Relative expression of Beclin1
G
Vehicle
MitoTEMPO
GOAPOL1
MitoSOX
mitoSOX fluorescence (RFU)
H
JC-1
Red: JC-1 aggregate; Green: JC-1 momomer
Green to red ratio
I
Akt
Cox IV
Histone3
Cyto
Crude mito
Nuc
J
qPCR quantification of cytoplasmic mtDNA
K
LC3
P62
Chloroquine
Stavation
L
M
Relative transcript level
Ndufa1
Cyc1
Sdhb
Uqcrc2
Uqcrb
Cox7b
Relative fluorescence of LC3-II
Relative fluorescence of P62

Figure S4. G2APOL1 induced mitophagy defect and mitochondrial dysfunction. Related to Figure 5.

A. Western blot analysis of mitochondrial markers (Cox4 and Hsp 60) in WT and *G2APOL1* ECs treated with vehicle, starvation (HBSS, 4h), or CCCP (40uM, 2h).
B. Densitometric quantification of Cox4 and HSP60 normalized to GAPDH. N = 3 independent experiments; *p < 0.05 and **p<0.01 vs. *Vehicle;* $^{\#}$p < 0.05, $^{\#\#\#}$p < 0.001 vs. indicated group.
C. Western blot analysis of the mitochondrial and cytosolic fraction of Parkin in WT and *G2APOL1* ECs treated as in A.
D. Densitometric quantification of mitochondrial fraction of Parkin normalized to cytosolic GAPDH. N = 3 independent experiments; **p < 0.01 and ***p<0.001 vs. *Vehicle;* $^{\#}$p < 0.05 vs. indicated group.
E. Immunoblot analysis using antibodies against LC3, p62, Beclin1 or GAPDH in WT and *G2APOL1* ECs treated with Vehicle, Chloroquine (100uM, 6h) and starvation (HBSS, 4h).
F. Densitometric quantification of LC3II, Beclin1 and p62 levels in panel I. N = 3 independent experiments; *p < 0.05 and **p<0.01 vs. *Vehicle;* $^{\#\#}$p < 0.01, $^{\#\#\#}$p < 0.001 vs. indicated group.
G. mtROS levels measured by MitoSOX staining in WT, *G0APOL1* and *G2APOL1* ECs treated with vehicle or mitoTEMPO (100nM, 4h). Representative images are shown. Scale bar=10µm. (Right panel) Quantification of the mtROS. ***p<0.001 vs *Vehicle*; $^{\#\#\#}$p < 0.001 vs. indicated group.
H. Mitochondrial membrane potential (Δψm) was determined by JC-1 assay in WT, G0APOL1 and G2APOL1 ECs treated with vehicle or CCCP (40uM, 2h), Scale bar = 10 µm. (Right panel) Quantification of the JC-1 fluorescence ratio in the experiment shown in panel C. ***p<0.001 vs *Vehicle*;
I. Expression of cell fraction markers Akt (cytosol), Cox4 (mitochondria) and Histone 3 (nucleus) by Western blot. N = 3 independent experiments.
J. Cytosolic mtDNA genes were normalized to respective nuclear Rpl13a and presented as fold enrichment over media-treated controls.
K. Representative immunofluorescence images of LC3 and p62 antibody staining in WT and *G2APOL* ECs treated with vehicle, starvation (HBSS, 4h) and chloroquine (100uM, 6h). Scale bar = 10 µm. (Right panel). Quantification of the LC3 and P62 in the experiment shown in panel H; *p<0.05, ***p<0.001 vs *WT*; $^{\#}$p < 0.05, $^{\#\#\#}$p < 0.001 vs. indicated group. N = 6 independent experiments (over 50 cells were counted in each case).
L. Heat map view representing the functional classification of differentially expressed genes in *G2APOL1* endothelial cells.
M. Relative mRNA levels of OXPHOS genes were evaluated in WT (N = 3), *G0APOL1* (N = 5) and *G2APOL1* (N = 5) ECs. *p < 0.05, **p<0.01, ***p<0.001 vs *WT*.

Figs5

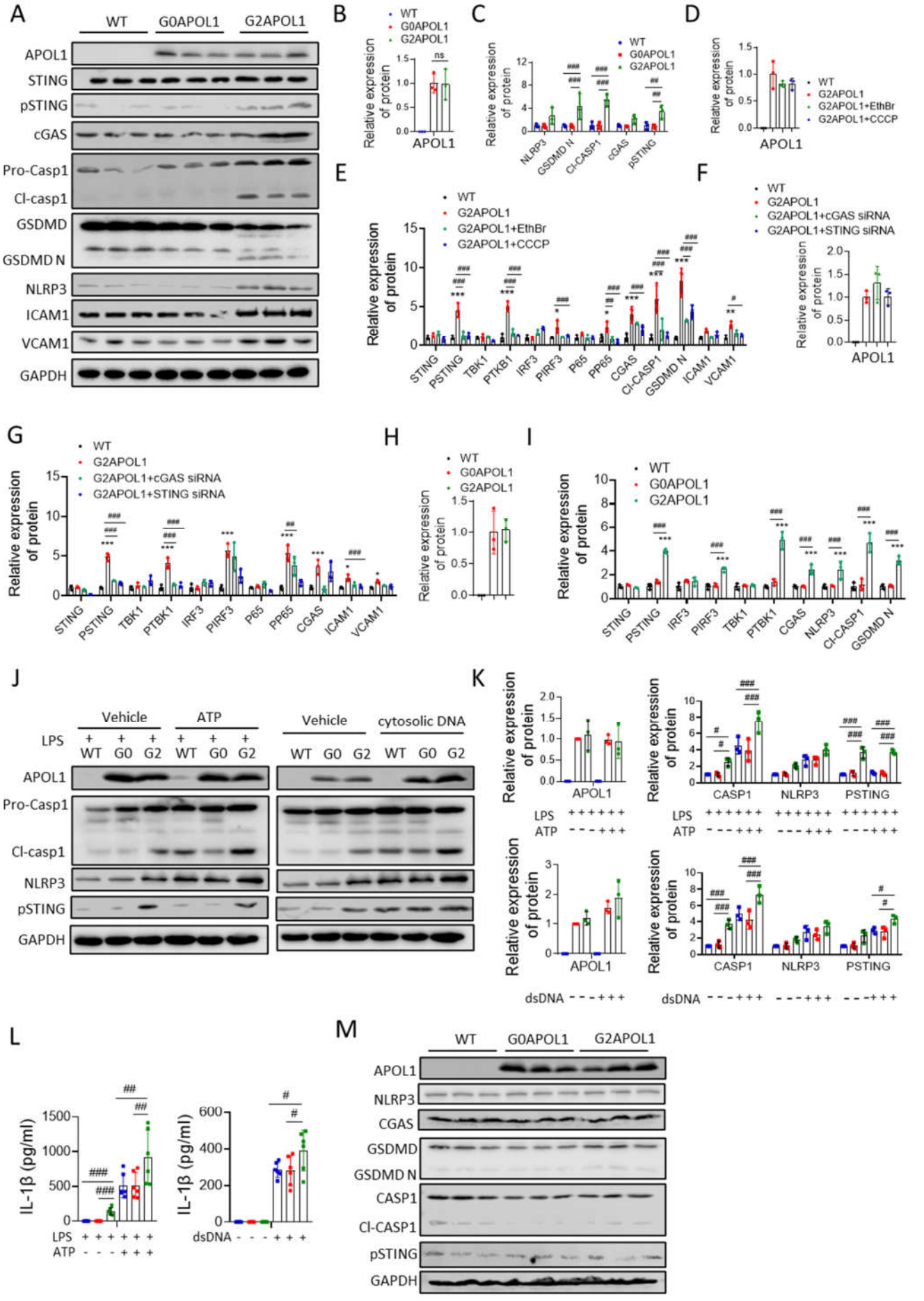
A
WT
G0APOL1
G2APOL1
APOL1
STING
pSTING
cGAS
Pro-Casp1
Cl-casp1
GSDMD
GSDMD N
NLRP3
ICAM1
VCAM1
GAPDH
B
Relative expression of protein
ns
APOL1
C
NLRP3
GSDMD N
Cl-CASP1
cGAS
pSTING
D
G2APOL1+EthBr
G2APOL1+CCCP
E
STING
PSTING
TBK1
PTKB1
IRF3
PIRF3
P65
PP65
CGAS
Cl-CASP1
GSDMD N
ICAM1
VCAM1
F
G2APOL1+cGAS siRNA
G2APOL1+STING siRNA
G
H
I
PTBK1
PIRF3
CASP1
J
Vehicle
ATP
cytosolic DNA
LPS
K
dsDNA
L
IL-1β (pg/ml)
M

Figure S5. Mitophagy defect in G2APOL1 ECs results in cytosolic mtDNA leakage, inflammasome and STING activation leading to an inflammatory, pro-adhesive endothelial phenotype. Related to Figure 6.

A. Protein expression of APOL1, ICAM1, VCAM1, inflammasome (NLRP3, GSDMD, CASP1) and cytosolic nucleotide sensors (STING, pSTING, cGAS) were analysed by immunoblotting in WT, *G0APOL1* and *G2APOL1* ECs.
B. Densitometric quantification of APOL1 in panel A, normalized to GAPDH. N = 3 independent experiments.
C. Densitometric quantification of ICAM1, VCAM1, NLRP3, GSDMD N, cl-Caspase1, cGAS and pSTING in panel A, normalized to GAPDH. $^{\#\#}p < 0.01$, $^{\#\#\#}p < 0.001$ vs. indicated group.
D. Densitometric quantification of APOL1 in figure 6A, normalized to GAPDH. N = 3 independent experiments.
E. Densitometric quantification of ICAM1, VCAM1, STING, pSTING, TBK1, pTBK1, IRF3, pIRF3, p65, P-P65, CGAS, cl-CASP1, and GSDMD N in Figure 6A, normalized to GAPDH. $^{*}p < 0.05$, $^{**}p<0.01$, $^{***}p<0.001$ vs. WT; $^{\#}p < 0.05$, $^{\#\#}p < 0.01$, and $^{\#\#\#}p < 0.001$ vs. indicated group.
F. Densitometric quantification of APOL1 in figure 6C, normalized to GAPDH. N = 3 independent experiments.
G. Densitometric quantification of ICAM1, VCAM1, STING, pSTING, TBK1, pTBK1, IRF3, pIRF3, P65, p-P65, and CGAS, in Figure 6C, normalized to GAPDH. N = 3 independent experiments; $^{*}p < 0.05$, $^{**}p<0.01$, $^{***}p<0.001$ vs. WT; $^{\#}p < 0.05$, $^{\#\#}p < 0.01$, and $^{\#\#\#}p < 0.001$ vs. indicated group.
H. Densitometric quantification of APOL1 in figure 6E, normalized to GAPDH. N = 3 independent experiments.
I. Densitometric quantification of STING, pSTING, TBK1, pTBK1, IRF3, pIRF3, CGAS, cl-CASP1, and GSDMD N in Figure 6E, normalized to GAPDH. N = 3 independent experiments; $^{*}p < 0.05$, $^{**}p<0.01$, $^{***}p<0.001$ vs. WT; $^{\#}p < 0.05$, $^{\#\#}p < 0.01$, and $^{\#\#\#}p < 0.001$ vs. indicated group.
J. (Left panel) WT, G0APOL1 and G2APOL1 ECs were incubated with LPS and ATP. (Right panel) ECs cells (WT, *G0APOL1* and *G2APOL1*) were transfected with DNA lysate isolated from damaged cells Protein expression of APOL1, pSTING, Caspase1 and NLRP3 were analysed by immunoblot analysis.
K. Densitometric quantification of APOL1, pSTING, Caspase1 and NLRP3 in panel J, normalized to GAPDH. N = 3 independent experiments; $^{*}p < 0.05$, $^{**}p<0.01$, $^{***}p<0.001$ vs. WT; $^{\#}p < 0.05$, $^{\#\#}p < 0.01$, and $^{\#\#\#}p < 0.001$ vs. indicated group.
L. Cell culture supernatant IL-1 beta of WT (N = 6), *G0APOL1*(N = 6) and *G2APOL1* (N = 6) ECs treated as panel J; $^{\#}p < 0.05$, $^{\#\#}p < 0.01$, and $^{\#\#\#}p < 0.001$ vs. indicated group.
M. Protein expression of NLRP3, CGAS, GSDMD, Caspase 1, pSTING and GAPDH were analysed by immunoblotting in liver of WT, liver/*G0APOL1* and liver/*G2APOL1* mice. N = 3 independent experiments.

Figs6

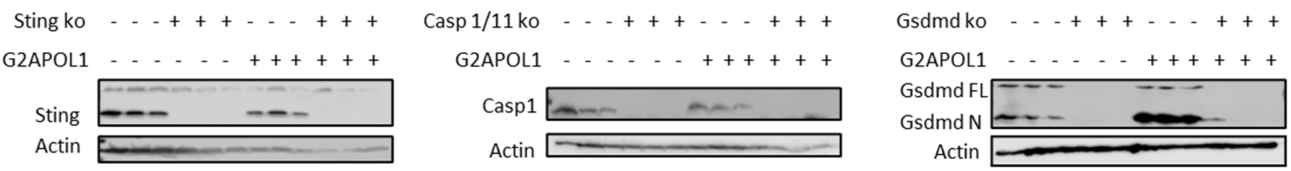
A
Sting ko
G2APOL1
Sting
Actin
Casp 1/11 ko
G2APOL1
Casp1
Actin
Gsdmd ko
G2APOL1
Gsdmd FL
Gsdmd N
Actin

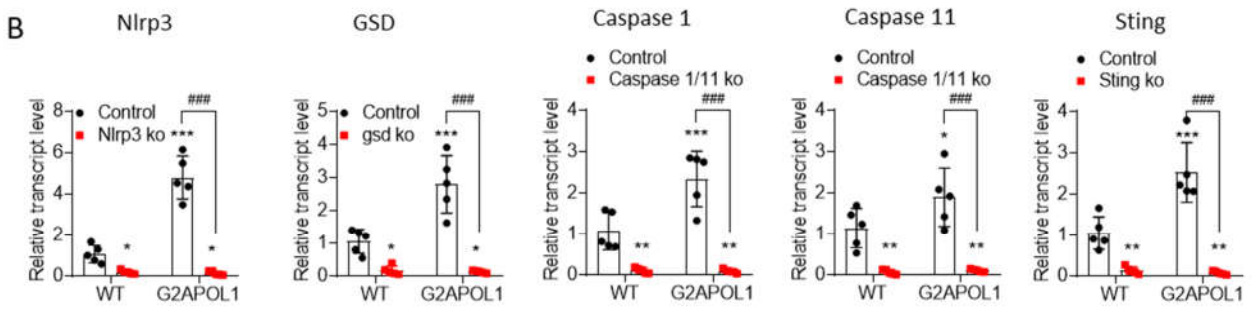
B
Nlrp3
GSD
Caspase 1
Caspase 11
Sting
Control
Nlrp3 ko
gsd ko
Caspase 1/11 ko
Sting ko
Relative transcript level
WT
G2APOL1

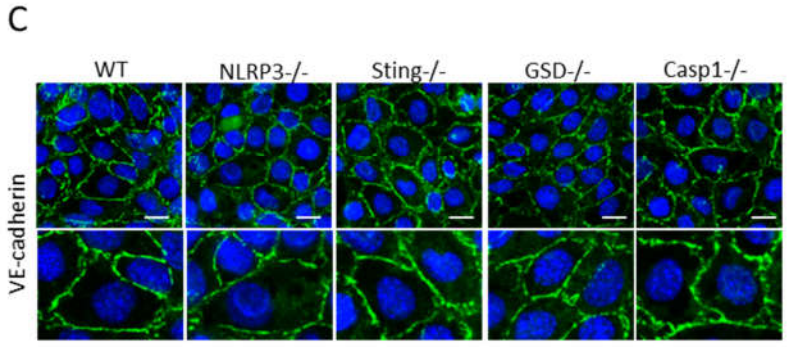
C
WT
NLRP3-/-
Sting-/-
GSD-/-
Casp1-/-
VE-cadherin

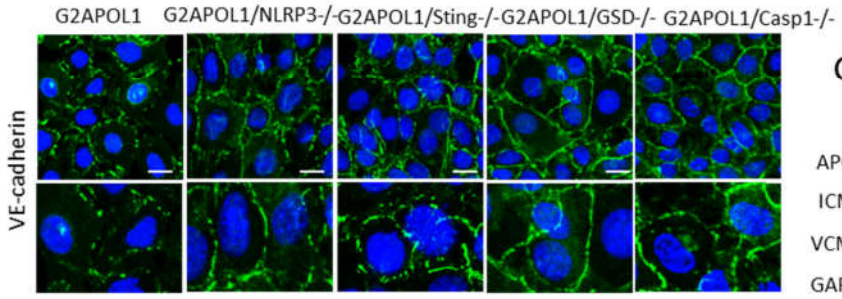
G2APOL1
G2APOL1/NLRP3-/-
G2APOL1/Sting-/-
G2APOL1/GSD-/-
G2APOL1/Casp1-/-
VE-cadherin

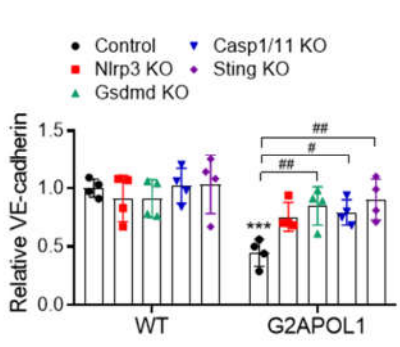
D
Control
Nlrp3 KO
Gsdmd KO
Casp1/11 KO
Sting KO
Relative VE-cadherin
WT
G2APOL1

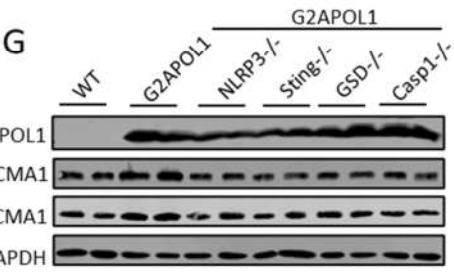
G
G2APOL1
WT
G2APOL1
NLRP3-/-
Sting-/-
GSD-/-
Casp1-/-
APOL1
ICMA1
VCMA1
GAPDH

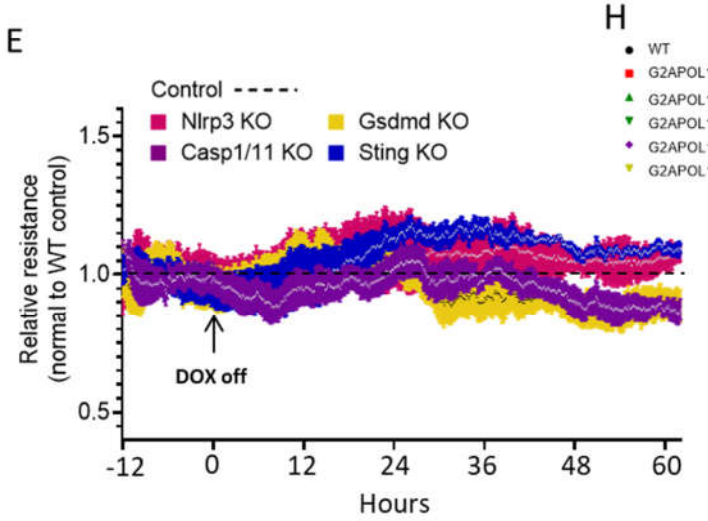
E
Control
Nlrp3 KO
Gsdmd KO
Casp1/11 KO
Sting KO
Relative resistance (normal to WT control)
DOX off
Hours

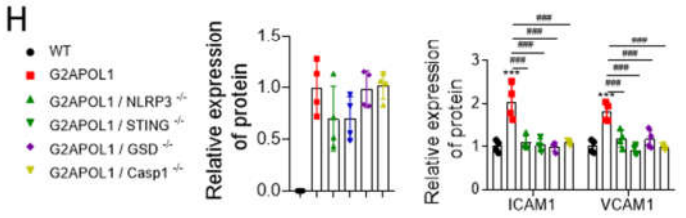
H
WT
G2APOL1
G2APOL1 / NLRP3 -/-
G2APOL1 / STING -/-
G2APOL1 / GSD -/-
G2APOL1 / Casp1 -/-
Relative expression of protein
ICAM1
VCAM1

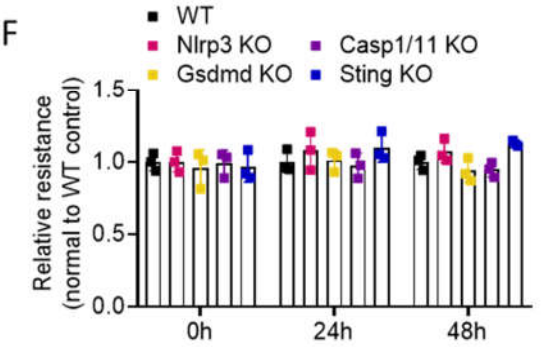
F
WT
Nlrp3 KO
Gsdmd KO
Casp1/11 KO
Sting KO
Relative resistance (normal to WT control)
0h
24h
48h

Figure S6. Genetic deletion of Nlrp3, Gsdmd, Caspase 1/11 or Sting in G2APOL1 transgenic mice. Related to Figure 7.

A. Western blots of whole lung lysates from *G2APOL1/Nlrp3 WT* and *G2APOL1/NLRP3 KO* mice, showing levels NLRP3, APOL1, caspase-1, cleaved caspase-1, caspase-11, cleaved caspase-11, and GAPDH.
B. Relative *Nlrp3*, *Gsdmd*, *Caspase* 1, *Caspase 11* and *Sting* transcript level in lung of WT/*Nlrp3*$^{-/-}$, WT/*Gsdmd*$^{-/-}$, WT/*Caspase 1/11*$^{-/-}$, WT/*Sting*$^{-/-}$, *G2APOL1/Nlrp3*$^{-/-}$*, G2APOL1/Gsdmd*$^{-/-}$*, G2APOL1/Caspase 1/11*$^{-/-}$*,* and *G2APOL1/Sting*$^{-/-}$ mice. *p<0.05, ***p<0.01, ***p<0.001 vs *WT control*; $^{\#\#\#}$p < 0.001 vs. indicated group.
C. Immunofluorescence analysis of VE-cadherin in indicated groups. Scale bar = 10 µm.
D. Quantification of VE-cadherin as shown in C. ***p<0.001 *vs* WT control; $^{\#}$p < 0.05, $^{\#\#}$p < 0.01 vs. indicated group.
E. TEER (measured in real time by ECIS) in ECs from WT, EC/*G2APOL1*, *Nlrp3*$^{-/-}$*/G2APOL, Gsdmd*$^{-/-}$*/G2APOL1, Casp 1/11*$^{-/-}$*/G2APOL1* and *STING*$^{-/-}$*/G2APOL1* mice. At each individual time point, TEER values were normalized to WT endothelial cells.
F. Relative TEER at 0 hr, 24 hrs and 48 hrs after removal of doxycycline (APOL1 expression).
G. Western blots of whole lung lysates from WT, EC/*G2APOL1, G2APOL1/Nlrp3*$^{-/-}$*, G2APOL1/Gsdmd*$^{-/-}$*, G2APOL1/Caspase 1/11*$^{-/-}$*,* and *G2APOL1/Sting*$^{-/-}$ mice, showing levels of APOL1, ICAM1, VCAM1 and GAPDH.
H. Densitometric quantification of APOL1, VCAM1 and ICAM1 in panel G, normalized to GAPDH. N = 4 independent experiments; ***p<0.001 vs. WT; and $^{\#\#\#}$p < 0.001 vs. indicated group.

Figs7

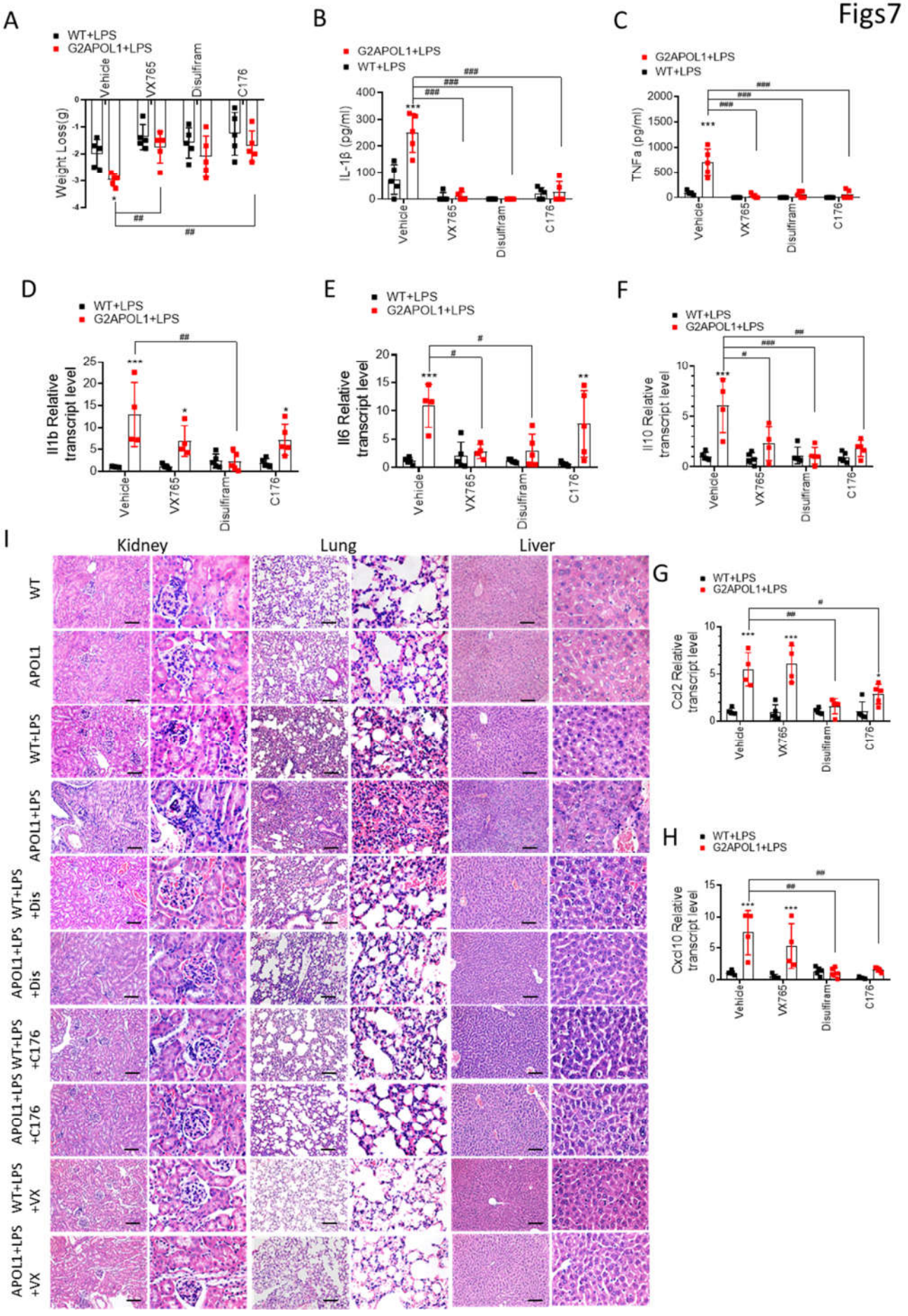
A
WT+LPS
G2APOL1+LPS
Vehicle
VX765
Disulfiram
C176
Weight Loss(g)
B
G2APOL1+LPS
WT+LPS
IL-1β (pg/ml)
C
G2APOL1+LPS
WT+LPS
TNFa (pg/ml)
D
WT+LPS
G2APOL1+LPS
Il1b Relative transcript level
E
WT+LPS
G2APOL1+LPS
Il6 Relative transcript level
F
WT+LPS
G2APOL1+LPS
Il10 Relative transcript level
I
Kidney
Lung
Liver
WT
APOL1
WT+LPS
APOL1+LPS
WT+LPS +Dis
APOL1+LPS +Dis
WT+LPS +C176
APOL1+LPS +C176
WT+LPS +VX
APOL1+LPS +VX
G
WT+LPS
G2APOL1+LPS
Cd2 Relative transcript level
H
WT+LPS
G2APOL1+LPS
Cxcl10 Relative transcript level

Figure S7. Pharmacological inhibition of GSDMD, Caspase 1 and STING improves LPS induced sepsis in EC/G2APOL1 mice. Related to Figure 7.

A. Weight loss 24 hours after intraperitoneal injection of LPS (6mg/kg) in groups (N =5) as indicated. *p<0.05, vs *WT+LPS*; $^{\#\#}$p < 0.01 vs. indicated group.
B. Serum interleukin 1 beta levels in groups (N =5) as indicated; ***p<0.001 vs *WT+LPS*; $^{\#\#\#}$p < 0.001 vs. indicated group.
C. Serum TNFα levels in groups (N =5) as indicated; ***p<0.001 vs *WT+LPS*; $^{\#\#\#}$p < 0.001 vs. indicated group.

D-H. Relative mRNA levels of *IL-1β*, interleukin 6 (*Il6*), interleukin 10 (*Il10*), *Ccl2* and C-X-C Motif Chemokine Ligand 10 (*Cxcl10*) in the lung of mice as indicated (N =5); *p<0.05, **p<0.01, ***p<0.001 vs *WT+LPS*; $^{\#}$p < 0.05, $^{\#\#}$p < 0.01 $^{\#\#\#}$p < 0.001 vs. indicated group.

I. Representative images of H&E-stained sections of kidneys, hearts, and lungs 24 hours after saline or LPS injection in WT, and EC/*G2APOL1* mice. Scale bar = 100μm

Table S1: Patient's characteristics in MESSI cohort. Related to Figure 1

Clinlical data	Non-AKI (N=26)	AKI (N=44)	P value
Age (y)	56.9 ± 16.5	63.2 ± 14.5	0.0998
Male, n%	14 (54%)	21 (48%)	0.6208
Black, n(%)	26 (100%)	44(100%)	ns
Hispanic, n(%)	2 (8%)	0 (0%)	0.0620
Mortality, n(%)	8 (30%)	18 (41%)	0.3962
BMI	26.3 ± 6.4	32.9 ± 10.7	0.0057
Apache III	73.5 ± 35.1	103.2 ± 37.2	0.0016

Data are expressed as medians, in parentheses percentages are given. Level of significance is set at $p<0.05$.
Related to Figure 1.

Table S2: Patient's characteristics in COVID19 cohort. Related to Figure 1

Clinlical data	Non-AKI (N=20)	AKI (N=10)	P value
Age (y)	55.6 ± 17.59	65.2 ± 20.94	0.1965
Male, n%	10	7	0.2974
White, n(%)	5 (25%)	1(10%)	0.3329
Black, n(%)	12 (60%)	7(70%)	0.5921
Other/unknown/Asian, n(%)	3 (15%)	2(20%)	0.7290
Mortality, n(%)	2 (10%)	3(30%)	0.1659
Admitted to ICU, n(%)	10 (50%)	6(60%)	0.6048

Data are expressed as medians, in parentheses percentages are given. Level of significance is set at $p<0.05$. **Related to Figure 1.**

Table S3: qPCR primer sequences. Related to STAR Methods. Related to STAR Methods

Gene		
Vcam1	Forward Primer	AGTTGGGGATTCGGTTGTTCT
	Reverse Primer	CCCCTCATTCCTTACCACCC
Icam1	Forward Primer	GTGATGCTCAGGTATCCATCCA
	Reverse Primer	CACAGTTCTCAAAGCACAGCG
Ccl2	Forward Primer	TTAAAAACCTGGATCGGAACCAA
	Reverse Primer	GCATTAGCTTCAGATTTACGGGT
GAPDH	Forward Primer	AGGTCGGTGTGAACGGATTTG
	Reverse Primer	TGTAGACCATGTAGTTGAGGTCA
Sdc1	Forward Primer	AACGGGCCTCAACAGTCAG
	Reverse Primer	CCGTGCGGATGAGATGTGA
Sdc2	Forward Primer	TGTGTCCGCAGAGACGAGAA
	Reverse Primer	GGAATCAGTTGGGATGTTGTCA
Sdc3	Forward Primer	AGAGGCCGGTGGATCTTGA
	Reverse Primer	CTCCTGCTCGAAGTAGCCAGA
Sdc4	Forward Primer	TTTGCCGTTTTCCTGATCCTG
	Reverse Primer	TTGCCCAAGTCGTAACTGCC
Hpse	Forward Primer	ACCGACGACGTGGTAGACTT
	Reverse Primer	GCAGGAGATAAGCCTCTAGCC
Hyal1	Forward Primer	ACCTGCTTCGCATCTCTACTC
	Reverse Primer	GGTTGGATACCACGGAACCTC
Hyal2	Forward Primer	AGATGTTTACCGACAGTCTTCAC
	Reverse Primer	TGACGTAACGGAGAGTGTTCAA
Mmp2	Forward Primer	CAAGTTCCCCGGCGATGTC
	Reverse Primer	TTCTGGTCAAGGTCACCTGTC
Mmp9	Forward Primer	CTGGACAGCCAGACACTAAAG
	Reverse Primer	CTCGCGGCAAGTCTTCAGAG
Mmp14	Forward Primer	CAGTATGGCTACCTACCTCCAG
	Reverse Primer	GCCTTGCCTGTCACTTGTAAA
Has1	Forward Primer	GGCGAGCACTCACGATCATC
	Reverse Primer	AGGAGTCCATAGCGATCTGAAG
Has2	Forward Primer	TGTGAGAGGTTTCTATGTGTCCT
	Reverse Primer	ACCGTACAGTCCAAATGAGAAGT
Sulf1	Forward Primer	TGTGTTCCACCGTTCGGTC
	Reverse Primer	CACATCCTGGTCGTCAGTGAG
Sulf2	Forward Primer	CTGCCACTATGGCTGCTGTC
	Reverse Primer	GTTGGGCCGGATGTTCCTG
Nos3	Forward Primer	GGCTGGGTTTAGGGCTGTG
	Reverse Primer	CTGAGGGTGTCGTAGGTGATG
Edn1	Forward Primer	GCACCGGAGCTGAGAATGG
	Reverse Primer	GTGGCAGAAGTAGACACACTC
Kim	Forward Primer	ACATATCGTGGAATCACAACGAC
	Reverse Primer	ACAAGCAGAAGATGGGCATTG
Ngal	Forward Primer	TGGCCCTGAGTGTCATGTG
	Reverse Primer	CTCTTGTAGCTCATAGATGGTGC
Il1b	Forward Primer	GCAACTGTTCCTGAACTCAACT
	Reverse Primer	ATCTTTTGGGGTCCGTCAACT
Il6	Forward Primer	TAGTCCTTCCTACCCCAATTTCC
	Reverse Primer	TTGGTCCTTAGCCACTCCTTC
Il10	Forward Primer	GCTCTTACTGACTGGCATGAG
	Reverse Primer	CGCAGCTCTAGGAGCATGTG
Cxcl10	Forward Primer	CCAAGTGCTGCCGTCATTTTC

	Reverse Primer	GGCTCGCAGGGATGATTTCAA
Ifnb	Forward Primer	CAGCTCCAAGAAAGGACGAAC
	Reverse Primer	GGCAGTGTAACTCTTCTGCA
Nlrp3	Forward Primer	ATTACCCGCCCGAGAAAGG
	Reverse Primer	TCGCAGCAAAGATCCACACAG
Gsdmd	Forward Primer	CCATCGGCCTTTGAGAAAGTG
	Reverse Primer	ACACATGAATAACGGGGTTTCC
Casp 1	Forward Primer	ACAAGGCACGGGACCTATG
	Reverse Primer	TCCCAGTCAGTCCTGGAAATG
Casp 11	Forward Primer	ACAAACACCCTGACAAACCAC
	Reverse Primer	CACTGCGTTCAGCATTGTTAAA
Sting	Forward Primer	GGTCACCGCTCCAAATATGTAG
	Reverse Primer	CAGTAGTCCAAGTTCGTGCGA
Cgas	Forward Primer	GAGGCGCGGAAAGTCGTAA
	Reverse Primer	TTGTCCGGTTCCTTCCTGGA
IFIT1	Forward Primer	CTGAGATGTCACTTCACATGGAA
	Reverse Primer	GTGCATCCCCAATGGGTTCT
IFITM1	Forward Primer	GACAGCCACCACAATCAACAT
	Reverse Primer	CCCAGGCAGCAGAAGTTCAT
mtATP6	Forward Primer	CAGTCCCCTCCCTAGGACTT
	Reverse Primer	TCAGAGCATTGGCCATAGAA
Rpl13a	Forward Primer	GGGCAGGTTCTGGTATTGGAT
	Reverse Primer	GGCTCGGAAATGGTAGGGG
Stat1	Forward Primer	TCACAGTGGTTCGAGCTTCAG
	Reverse Primer	GCAAACGAGACATCATAGGCA
Irf7	Forward Primer	GAGACTGGCTATTGGGGGAG
	Reverse Primer	GACCGAAATGCTTCCAGGG
Isg15	Forward Primer	GGTGTCCGTGACTAACTCCAT
	Reverse Primer	TGGAAAGGGTAAGACCGTCCT
Podxl	Forward Primer	GCCACCAAAGTGCCACAAC
	Reverse Primer	CGGCATAGATGGAGATTGGGTT
Ndufa1	Forward Primer	ATGTGGTTCGAGATTCTCCCT
	Reverse Primer	TGGTACTGAACACGAGCAACT
Cyc1	Forward Primer	CAGCTTCCATTGCGGACAC
	Reverse Primer	GGCACTCACGGCAGAATGAA
Sdhb	Forward Primer	AATTTGCCATTTACCGATGGGA
	Reverse Primer	AGCATCCAACACCATAGGTCC
Uqcrc2	Forward Primer	AAAGTTGCCCCGAAGGTTAAA
	Reverse Primer	GAGCATAGTTTTCCAGAGAAGCA
Uqcrb	Forward Primer	GGCCGATCTGCTGTTTCAG
	Reverse Primer	CATCTCGCATTAACCCCAGTT
Cox7b	Forward Primer	TTGCCCTTAGCCAAAAACGC
	Reverse Primer	TCATGGAAACTAGGTGCCCTC

Data S1. VA Million Veteran Program: Core Acknowledgement for Publications

Updated December 10, 2020. Related to figure 1.

MVP Executive Committee

- Co-Chair: J. Michael Gaziano, M.D., M.P.H.
  VA Boston Healthcare System, 150 S. Huntington Avenue, Boston, MA 02130
- Co-Chair: Sumitra Muralidhar, Ph.D.
  US Department of Veterans Affairs, 810 Vermont Avenue NW, Washington, DC 20420
- Rachel Ramoni, D.M.D., Sc.D., Chief VA Research and Development Officer
  US Department of Veterans Affairs, 810 Vermont Avenue NW, Washington, DC 20420
- Jean Beckham, Ph.D.
  Durham VA Medical Center, 508 Fulton Street, Durham, NC 27705
- Kyong-Mi Chang, M.D.
  Philadelphia VA Medical Center, 3900 Woodland Avenue, Philadelphia, PA 19104
- Christopher J. O'Donnell, M.D., M.P.H.
  VA Boston Healthcare System, 150 S. Huntington Avenue, Boston, MA 02130
- Philip S. Tsao, Ph.D.
  VA Palo Alto Health Care System, 3801 Miranda Avenue, Palo Alto, CA 94304
- James Breeling, M.D., Ex-Officio
  US Department of Veterans Affairs, 810 Vermont Avenue NW, Washington, DC 20420
- Grant Huang, Ph.D., Ex-Officio
  US Department of Veterans Affairs, 810 Vermont Avenue NW, Washington, DC 20420
- Juan P. Casas, M.D., Ph.D., Ex-Officio
  VA Boston Healthcare System, 150 S. Huntington Avenue, Boston, MA 02130

MVP Program Office

- Sumitra Muralidhar, Ph.D.
  US Department of Veterans Affairs, 810 Vermont Avenue NW, Washington, DC 20420
- Jennifer Moser, Ph.D.
  US Department of Veterans Affairs, 810 Vermont Avenue NW, Washington, DC 20420

MVP Recruitment/Enrollment

- Recruitment/Enrollment Director/Deputy Director, Boston – Stacey B. Whitbourne, Ph.D.; Jessica V. Brewer, M.P.H.
  VA Boston Healthcare System, 150 S. Huntington Avenue, Boston, MA 02130
- MVP Coordinating Centers

    - Clinical Epidemiology Research Center (CERC), West Haven – Mihaela Aslan, Ph.D.
      West Haven VA Medical Center, 950 Campbell Avenue, West Haven, CT 06516
    - Cooperative Studies Program Clinical Research Pharmacy Coordinating Center, Albuquerque – Todd Connor, Pharm.D.; Dean P. Argyres, B.S., M.S.
      New Mexico VA Health Care System, 1501 San Pedro Drive SE, Albuquerque, NM 87108
    - Genomics Coordinating Center, Palo Alto – Philip S. Tsao, Ph.D.
      VA Palo Alto Health Care System, 3801 Miranda Avenue, Palo Alto, CA 94304
    - MVP Boston Coordinating Center, Boston - J. Michael Gaziano, M.D., M.P.H.
      VA Boston Healthcare System, 150 S. Huntington Avenue, Boston, MA 02130
    - MVP Information Center, Canandaigua – Brady Stephens, M.S.
      Canandaigua VA Medical Center, 400 Fort Hill Avenue, Canandaigua, NY 14424
- VA Central Biorepository, Boston – Mary T. Brophy M.D., M.P.H.; Donald E. Humphries, Ph.D.; Luis E. Selva, Ph.D.
  VA Boston Healthcare System, 150 S. Huntington Avenue, Boston, MA 02130
- MVP Informatics, Boston – Nhan Do, M.D.; Shahpoor (Alex) Shayan, M.S.
  VA Boston Healthcare System, 150 S. Huntington Avenue, Boston, MA 02130
- MVP Data Operations/Analytics, Boston – Kelly Cho, M.P.H., Ph.D.
  VA Boston Healthcare System, 150 S. Huntington Avenue, Boston, MA 02130
- Director of Regulatory Affairs – Lori Churby, B.S.
  VA Palo Alto Health Care System, 3801 Miranda Avenue, Palo Alto, CA 94304

MVP Science

- Science Operations – Christopher J. O'Donnell, M.D., M.P.H.
  VA Boston Healthcare System, 150 S. Huntington Avenue, Boston, MA 02130
- Genomics Core – Christopher J. O'Donnell, M.D., M.P.H.; Saiju Pyarajan Ph.D.
  VA Boston Healthcare System, 150 S. Huntington Avenue, Boston, MA 02130
  Philip S. Tsao, Ph.D.
  VA Palo Alto Health Care System, 3801 Miranda Avenue, Palo Alto, CA 94304
- Data Core – Kelly Cho, M.P.H, Ph.D.
  VA Boston Healthcare System, 150 S. Huntington Avenue, Boston, MA 02130
- VA Informatics and Computing Infrastructure (VINCI) – Scott L. DuVall, Ph.D.
  VA Salt Lake City Health Care System, 500 Foothill Drive, Salt Lake City, UT 84148
- Data and Computational Sciences – Saiju Pyarajan, Ph.D.
  VA Boston Healthcare System, 150 S. Huntington Avenue, Boston, MA 02130
- Statistical Genetics – Elizabeth Hauser, Ph.D.
  Durham VA Medical Center, 508 Fulton Street, Durham, NC 27705
  Yan Sun, Ph.D.
  Atlanta VA Medical Center, 1670 Clairmont Road, Decatur, GA 30033

Hongyu Zhao, Ph.D.
West Haven VA Medical Center, 950 Campbell Avenue, West Haven, CT 06516

Current MVP Local Site Investigators

- Atlanta VA Medical Center (Peter Wilson, M.D.)
  1670 Clairmont Road, Decatur, GA 30033
- Bay Pines VA Healthcare System (Rachel McArdle, Ph.D.)
  10,000 Bay Pines Blvd Bay Pines, FL 33744
- Birmingham VA Medical Center (Louis Dellitalia, M.D.)
  700 S. 19th Street, Birmingham AL 35233
- Central Western Massachusetts Healthcare System (Kristin Mattocks, Ph.D., M.P.H.)
  421 North Main Street, Leeds, MA 01053
- Cincinnati VA Medical Center (John Harley, M.D., Ph.D.)
  3200 Vine Street, Cincinnati, OH 45220
- Clement J. Zablocki VA Medical Center (Jeffrey Whittle, M.D., M.P.H.)
  5000 West National Avenue, Milwaukee, WI 53295
- VA Northeast Ohio Healthcare System (Frank Jacono, M.D.)
  10701 East Boulevard, Cleveland, OH 44106
- Durham VA Medical Center (Jean Beckham, Ph.D.)
  508 Fulton Street, Durham, NC 27705
- Edith Nourse Rogers Memorial Veterans Hospital (John Wells., Ph.D.)
  200 Springs Road, Bedford, MA 01730
- Edward Hines, Jr. VA Medical Center (Salvador Gutierrez, M.D.)
  5000 South 5th Avenue, Hines, IL 60141
- Veterans Health Care System of the Ozarks (Gretchen Gibson, D.D.S., M.P.H.)
  1100 North College Avenue, Fayetteville, AR 72703
- Fargo VA Health Care System (Kimberly Hammer, Ph.D.)
  2101 N. Elm, Fargo, ND 58102
- VA Health Care Upstate New York (Laurence Kaminsky, Ph.D.)
  113 Holland Avenue, Albany, NY 12208
- New Mexico VA Health Care System (Gerardo Villareal, M.D.)
  1501 San Pedro Drive, S.E. Albuquerque, NM 87108
- VA Boston Healthcare System (Scott Kinlay, M.B.B.S., Ph.D.)
  150 S. Huntington Avenue, Boston, MA 02130
- VA Western New York Healthcare System (Junzhe Xu, M.D.)
  3495 Bailey Avenue, Buffalo, NY 14215-1199
- Ralph H. Johnson VA Medical Center (Mark Hamner, M.D.)
  109 Bee Street, Mental Health Research, Charleston, SC 29401
- Columbia VA Health Care System (Roy Mathew, M.D.)
  6439 Garners Ferry Road, Columbia, SC 29209

- VA North Texas Health Care System (Sujata Bhushan, M.D.)
  4500 S. Lancaster Road, Dallas, TX 75216
- Hampton VA Medical Center (Pran Iruvanti, D.O., Ph.D.)
  100 Emancipation Drive, Hampton, VA 23667
- Richmond VA Medical Center (Michael Godschalk, M.D.)
  1201 Broad Rock Blvd., Richmond, VA 23249
- Iowa City VA Health Care System (Zuhair Ballas, M.D.)
  601 Highway 6 West, Iowa City, IA 52246-2208
- Eastern Oklahoma VA Health Care System (Douglas Ivins, M.D.)
  1011 Honor Heights Drive, Muskogee, OK 74401
- James A. Haley Veterans' Hospital (Stephen Mastorides, M.D.)
  13000 Bruce B. Downs Blvd, Tampa, FL 33612
- James H. Quillen VA Medical Center (Jonathan Moorman, M.D., Ph.D.)
  Corner of Lamont & Veterans Way, Mountain Home, TN 37684
- John D. Dingell VA Medical Center (Saib Gappy, M.D.)
  4646 John R Street, Detroit, MI 48201
- Louisville VA Medical Center (Jon Klein, M.D., Ph.D.)
  800 Zorn Avenue, Louisville, KY 40206
- Manchester VA Medical Center (Nora Ratcliffe, M.D.)
  718 Smyth Road, Manchester, NH 03104
- Miami VA Health Care System (Hermes Florez, M.D., Ph.D.)
  1201 NW 16th Street, 11 GRC, Miami FL 33125
- Michael E. DeBakey VA Medical Center (Olaoluwa Okusaga, M.D.)
  2002 Holcombe Blvd, Houston, TX 77030
- Minneapolis VA Health Care System (Maureen Murdoch, M.D., M.P.H.)
  One Veterans Drive, Minneapolis, MN 55417
- N. FL/S. GA Veterans Health System (Peruvemba Sriram, M.D.)
  1601 SW Archer Road, Gainesville, FL 32608
- Northport VA Medical Center (Shing Shing Yeh, Ph.D., M.D.)
  79 Middleville Road, Northport, NY 11768
- Overton Brooks VA Medical Center (Neeraj Tandon, M.D.)
  510 East Stoner Ave, Shreveport, LA 71101
- Philadelphia VA Medical Center (Darshana Jhala, M.D.)
  3900 Woodland Avenue, Philadelphia, PA 19104
- Phoenix VA Health Care System (Samuel Aguayo, M.D.)
  650 E. Indian School Road, Phoenix, AZ 85012
- Portland VA Medical Center (David Cohen, M.D.)
  3710 SW U.S. Veterans Hospital Road, Portland, OR 97239
- Providence VA Medical Center (Satish Sharma, M.D.)
  830 Chalkstone Avenue, Providence, RI 02908

- Richard Roudebush VA Medical Center (Suthat Liangpunsakul, M.D., M.P.H.)
  1481 West 10th Street, Indianapolis, IN 46202
- Salem VA Medical Center (Kris Ann Oursler, M.D.)
  1970 Roanoke Blvd, Salem, VA 24153
- San Francisco VA Health Care System (Mary Whooley, M.D.)
  4150 Clement Street, San Francisco, CA 94121
- South Texas Veterans Health Care System (Sunil Ahuja, M.D.)
  7400 Merton Minter Boulevard, San Antonio, TX 78229
- Southeast Louisiana Veterans Health Care System (Joseph Constans, Ph.D.)
  2400 Canal Street, New Orleans, LA 70119
- Southern Arizona VA Health Care System (Paul Meyer, M.D., Ph.D.)
  3601 S 6th Avenue, Tucson, AZ 85723
- Sioux Falls VA Health Care System (Jennifer Greco, M.D.)
  2501 W 22nd Street, Sioux Falls, SD 57105
- St. Louis VA Health Care System (Michael Rauchman, M.D.)
  915 North Grand Blvd, St. Louis, MO 63106
- Syracuse VA Medical Center (Richard Servatius, Ph.D.)
  800 Irving Avenue, Syracuse, NY 13210
- VA Eastern Kansas Health Care System (Melinda Gaddy, Ph.D.)
  4101 S 4th Street Trafficway, Leavenworth, KS 66048
- VA Greater Los Angeles Health Care System (Agnes Wallbom, M.D., M.S.)
  11301 Wilshire Blvd, Los Angeles, CA 90073
- VA Long Beach Healthcare System (Timothy Morgan, M.D.)
  5901 East 7th Street Long Beach, CA 90822
- VA Maine Healthcare System (Todd Stapley, D.O.)
  1 VA Center, Augusta, ME 04330
- VA New York Harbor Healthcare System (Scott Sherman, M.D., M.P.H.)
  423 East 23rd Street, New York, NY 10010
- VA Pacific Islands Health Care System (George Ross, M.D.)
  459 Patterson Rd, Honolulu, HI 96819
- VA Palo Alto Health Care System (Philip Tsao, Ph.D.)
  3801 Miranda Avenue, Palo Alto, CA 94304-1290
- VA Pittsburgh Health Care System (Patrick Strollo, Jr., M.D.)
  University Drive, Pittsburgh, PA 15240
- VA Puget Sound Health Care System (Edward Boyko, M.D.)
  1660 S. Columbian Way, Seattle, WA 98108-1597
- VA Salt Lake City Health Care System (Laurence Meyer, M.D., Ph.D.)
  500 Foothill Drive, Salt Lake City, UT 84148
- VA San Diego Healthcare System (Samir Gupta, M.D., M.S.C.S.)
  3350 La Jolla Village Drive, San Diego, CA 92161

- VA Sierra Nevada Health Care System (Mostaqul Huq, Pharm.D., Ph.D.)
  975 Kirman Avenue, Reno, NV 89502
- VA Southern Nevada Healthcare System (Joseph Fayad, M.D.)
  6900 North Pecos Road, North Las Vegas, NV 89086
- VA Tennessee Valley Healthcare System (Adriana Hung, M.D., M.P.H.)
  1310 24th Avenue, South Nashville, TN 37212
- Washington DC VA Medical Center (Jack Lichy, M.D., Ph.D.)
  50 Irving St, Washington, D. C. 20422
- W.G. (Bill) Hefner VA Medical Center (Robin Hurley, M.D.)
  1601 Brenner Ave, Salisbury, NC 28144
- White River Junction VA Medical Center (Brooks Robey, M.D.)
  163 Veterans Drive, White River Junction, VT 05009
- William S. Middleton Memorial Veterans Hospital (Robert Striker, M.D., Ph.D.)
  2500 Overlook Terrace, Madison, WI 53705